

# Unraveling Responsiveness of Chained BFT Consensus with Network Delay

Yining Tang, Qihang Luo, Runchao Han, Jianyu Niu, *Member, IEEE*,  
Chen Feng, *Member, IEEE*, Yinqian Zhang, *Member, IEEE*

**Abstract**—With the advancement of blockchain technology, chained Byzantine Fault Tolerant (BFT) protocols have been increasingly adopted in practical systems, making their performance a crucial aspect of the study. In this paper, we introduce a unified framework utilizing Markov Decision Processes (MDP) to model and assess the performance of three prominent chained BFT protocols. Our framework effectively captures complex adversarial behaviors, focusing on two key performance metrics: chain growth and commitment rate. We implement the optimal attack strategies obtained from MDP analysis on an existing evaluation platform for chained BFT protocols and conduct extensive experiments under various settings to validate our theoretical results. Through rigorous theoretical analysis and thorough practical experiments, we provide an in-depth evaluation of chained BFT protocols under diverse attack scenarios, uncovering optimal attack strategies. Contrary to conventional belief, our findings reveal that while responsiveness can enhance performance, it is not universally beneficial across all scenarios. This work not only deepens our understanding of chained BFT protocols, but also offers valuable insights and analytical tools that can inform the design of more robust and efficient protocols.

**Index Terms**—Chained BFT, Responsiveness, MDP, Attack strategy, Performance metrics.

## I. INTRODUCTION

The growing popularity of decentralized applications, including global payments [1], [2], DeFi [3], and online gaming [4], has revitalized interest in Byzantine Fault Tolerant (BFT) consensus. Recently, a family of chained BFT protocols utilizing the chaining structure of blockchains has attracted extensive attention for their ability to support large-scale decentralized applications. Notable examples include Tendermint [5], Casper FFG [6], HotStuff [7], Streamlet [8], Fast-HotStuff [9], and HotStuff-2 [10]. These protocols have been used in tens of blockchains, both permissioned (*e.g.*, XuperChain [11] and Hyperchain [12]) and permissionless (*e.g.*, Ethereum 2.0 [13], Aptos [14], Cypherium [15], Flow [16], Zilliqa 2.0 [17], and DeSo [18]).

Tendermint [5] and Casper FFG [6] are among the first generations of chained BFT protocols that utilize chain structure

Yining Tang, Qihang Luo, Jianyu Niu, and Yinqian Zhang are with the Research Institute of Trustworthy Autonomous Systems and the Department of Computer Science and Engineering, Southern University of Science and Technology, Shenzhen, China. Email: tangyn2018@mail.sustech.edu.cn, 12110425@mail.sustech.edu.cn, niujy@sustech.edu.cn and yinqianz@acm.org.

Runchao Han is Babylon Labs. E-mail: runchao@babylonlabs.io.

Chen Feng is with Blockchain@UBC and the School of Engineering, The University of British Columbia (Okanagan Campus), Kelowna, BC, Canada. Email: chen.feng@ubc.ca.

and pipelining techniques to realize linear message complexity and improve system efficiency, respectively. However, they cannot guarantee responsiveness, by which a designated leader can drive nodes to reach a consensus in time depending only on the actual message delays (denoted as  $\delta$ ), independent of any known upper bound delays (denoted as  $\Delta$ ). The upper bound delay represents the worst-case time for messages to propagate over the network, typically set to be more than an order of magnitude larger than the actual delay. Thus, achieving responsiveness is a hallmark of practical BFT protocols, as claimed in [7]. Due to its importance, subsequent chained BFT protocols such as chained HotStuff (CHS) and Fast-HotStuff (FHS) adopt different designs to achieve it. Specifically, CHS extends two-phase message exchanges to three-phase exchanges, whereas FHS requires blocks to include QCs (*i.e.*, a set of collected messages from more than two-thirds of nodes to denote the highest block they have seen). Despite the introduced protocol overhead, one common belief is that responsiveness can significantly enhance performance, guiding all following designs [10], [19], [20].

Unfortunately, the responsiveness belief behind chained BFT protocols has not been carefully examined. The prior benchmarks [21]–[24] try to evaluate the performance (*i.e.*, throughput and latency) of chained BFT protocols under various experimental settings. However, they mainly evaluate performance in the ideal cases, *i.e.*, all nodes follow the protocol. Studies [25]–[27] have shown that in chained HotStuff, an adversary can strategically fork uncommitted blocks from honest leaders to weaken the system performance. Since chained BFT protocols are usually deployed among distrusting nodes, it is important to analyze or evaluate the impact of responsiveness on performance under attacks. More importantly, to fairly compare chained BFT with/without responsiveness, we should determine their worst performance and the associated optimal adversarial attack strategies. To our knowledge, none of the existing studies can achieve this.

In this paper, we propose a comprehensive framework to analyze the impact of responsiveness on system performance. With the framework, we can analyze the performance of existing chained BFT protocols, *i.e.*, chained HotStuff (CHS), Two-Chain HotStuff (2CHS), and Fast-HotStuff (FHS) as well as other chained BFT protocols, under attacks. Instead of using traditional throughput and latency metrics [21]–[24], we propose two customized performance metrics: *chain growth*, which is the rate at which honest blocks are added to the main chain, reflecting the system’s capacity to process transactions, and *commitment rate*, which indicates the frequency of block

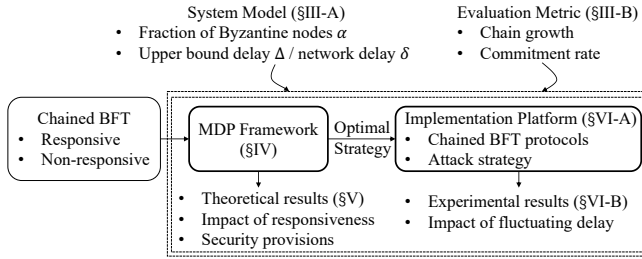


Figure 1: An overview of the proposed framework.

commitment events on the main chain, showing the speed of transaction confirmation. Both metrics focus on the blocks instead of transactions (usually used to measure traditional throughput and latency metrics), which enables us to ignore unnecessary details like transaction batch size and block size. Thus, these two metrics not only reflect performance under attack scenarios but also are easier to trace in Markov Decision Processes (MDP) modeling.

Our framework consists of two key components: (i) an MDP-based analytical model and (ii) an evaluation platform, as shown in Fig. 1. The first component enables us to explore optimal attack strategies in chained BFT protocols by considering factors such as the fraction of Byzantine nodes, the impact of network delay, and various consensus rules. MDP provides a mathematical framework for simulating and analyzing decision processes in random environments, making it highly suitable for quantifying the impact of arbitrary behaviors of random-selected adversarial leaders on protocol performance.

With this MDP framework, we can fairly compare the performance of responsive and non-responsive chained BFT protocols under diverse attack scenarios. Although MDP has been used to analyze the performance and security of the Nakamoto-style consensus [28]–[31], its application to chained BFT protocols remains challenging due to fundamental design differences. Our work requires reconstructing the MDP model to accommodate the chained BFT consensus, which demands an in-depth comprehension of both MDP tools and the details of chained BFT protocols. As one of our contributions, we properly simplify the system state and constrain adversary actions to facilitate MDP modeling of various chained BFT protocols.

The second component enables us to implement the optimal attack strategies identified by the MDP modeling on some implementation platforms of chained BFT protocols. In this work, we adopt the open-sourced Bamboo platform [32], which supports CHS, FHS, and Streamlet [8]. Although Bamboo also supports performance evaluation under attacks, these strategies are straightforward and so cannot provide a fair comparison between chained BFT protocols. Our extension to Bamboo not only can validate the theoretical results from MDP modeling, but also can evaluate performance with consideration of more factors of practical systems such as fluctuating network delay.

Our work provides a way to holistically compare the impact of responsiveness on the system performance. For instance, when the fraction of Byzantine nodes is small, responsive protocols can achieve better chain growth and commitment

rates. Our key findings are summarized as follows:

- *Finding 1:* The chain growth and commitment rate of all three chosen protocols significantly degrade under attacks, especially with a higher fraction of Byzantine nodes. Responsiveness improves the performance of chained BFT protocols at lower fractions of Byzantine nodes but provides diminishing returns as the fraction increases.
- *Finding 2:* While responsiveness is crucial, its implementation does not always improve protocol performance. The design needs to consider specific protocol needs and the presence of attacks.
- *Finding 3:* The experiments affirm the framework’s validity, demonstrating that chain growth and commitment rate maintain robustness even under realistic network conditions.

**Contributions.** The contributions of this paper are listed below.

- We propose an evaluation framework with two metrics, chain growth and commitment rate, to systematically analyze the performance of chained BFT protocols.
- We model and evaluate three representative chained BFT protocols under different fractions of Byzantine nodes based on the proposed framework. We obtain the optimal theoretical results and attack strategies. Through an analysis of the results under different fractions, we find the impact of responsiveness on protocol performance
- We conduct extensive empirical experiments to validate the theoretical framework in real-world settings, examining the impact of network delay fluctuations on protocol performance. The integration of theoretical analysis and empirical validation enhances the reliability of our findings.

*Code availability.* The source code of MDP and evaluation framework are provided in [33] and [34], respectively.

**Roadmap.** Sec. II introduces background and related work on chained BFT protocols. Sec. III provides the system model and metrics. Sec. IV presents MDP model of chained BFT protocols. The theoretical results of MDP model and experimental results are provided in Sec. V and Sec. VI, respectively. We introduce extensions of the framework in Sec. VII and conclude the paper in Sec. VIII.

## II. BACKGROUND AND RELATED WORK

We first provide the background of chained BFT protocols and the associated performance issues. Then, we review prior studies on the performance analysis of chained BFT protocols.

### A. Chained BFT Consensus

Chained BFT consensus represents a family of BFT protocols that leverage the chain structure for better performance and scalability [7]–[9]. Chained BFT protocols run in views, in which a designated replica (called the leader) coordinates with others to vote for its block, as shown in Fig. 2. Specifically, each view can be further divided into two stages: the leader-based stage and the view-change stage. In the former, the leader proposes a new block to extend previous blocks, *i.e.*, forming a chain, according to the proposing rule. Then, other

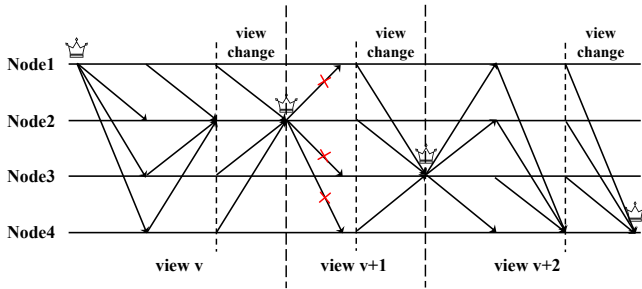


Figure 2: The consensus process of chained BFT protocols.

nodes append the first valid block from the leader to their chain and update the local state of the locked block. Later, they vote for the block by the voting rule. Once a block has enough votes (from more than  $2/3$  of the nodes), it forms a Quorum Certificate (QC) and is certified. Node follows the committing rule to check whether an uncommitted block in the chain can be committed. Note that once a block is committed, its uncommitted ancestor blocks are also committed.

In the view-change stage, nodes safely wedge to the next round if the leader is faulty or the proposed block’s quorum certificate is not formed before the timeout. This stage is also referred to as Pacemaker [7]. It is crucial for the *liveness* property, by which honest clients’ transactions are eventually included in committed blocks. Meanwhile, chained BFT protocols also need to ensure the *safety property*, by which honest nodes accept the same committed chain of blocks, referred to as the *main chain*—a key concept that will be used in our analysis. In other words, a block is included in the main chain once being committed.

**Responsiveness.** The responsiveness property ensures that a designated leader can drive nodes to reach consensus solely at the speed determined by actual network delays ( $\delta$ ), without relying on any predefined upper bound on delays ( $\Delta$ ). Specifically, the upper bound delay  $\Delta$  guarantees message delivery between any two honest nodes after Global Stabilization Time (GST), concerned with system liveness, whereas the network delay  $\delta$  directly affects the system performance. Thus, responsiveness foregoes a hallmark of practical BFT protocols, as claimed in [7].

Due to its importance, many chained BFT protocols adopt different designs to achieve responsiveness. Specifically, Two-Chain HotStuff (2CHS) formulated from Tendermint [5] and Casper FFG [6] is the original chained BFT protocol without responsiveness. Later, chained HotStuff (CHS) extends two-phase message exchanges to three-phase exchanges. Fast-HotStuff (FHS) introduces the latest QC proof and achieves responsiveness within two-phase exchanges. FHS also optimizes the protocol to skip view change in the happy path. As said previously, achieving responsiveness or not directly affects system performance, further determining their practicality. Thus, exploring the impact of responsiveness or how to achieve better responsiveness is an important question.

**Performance under attacks.** The performance of BFT protocols is usually measured in terms of throughput and latency [35], [36]. Throughput refers to the number of trans-

Table I: Summary of prior frameworks to evaluate the performance of chained BFT protocols under attacks.

Framework	Methodology		Optimal Strategy
	Experimental	Theoretical	
[21]–[24], [26], [27]	✓	✗	✗
[25]	✗	✓	✗
This work	✓	✓	✓

actions that can be processed per unit of time, while latency measures the time taken to reach consensus on a transaction. Applying BFT protocols to blockchain introduces the concept of block, which leads to a greater focus on honest blocks.

The performance of chained BFT protocols can be affected by Byzantine nodes. A Byzantine leader may intentionally cause delays in the protocol. For example, it can put off the decision-making or vote-collecting process, leading to slow consensus progress before triggering a timeout. It can also remain silent [27] or propose invalid blocks, causing the entire consensus process to stall until a timeout occurs. The Byzantine leader can also exclude honest blocks from the chain or disrupt the committing rule of blocks [25], causing the transactions in the block to be delayed. Therefore, it is essential to identify potential vulnerabilities and then measure their impact on performance.

## B. Related Work

We first introduce some state-of-the-art chained BFT protocols. Then, we review existing studies to analyze the performance of chained BFT protocols, as well as MDP modeling of blockchain consensus protocols. Table I lists existing benchmarks and evaluation frameworks of chained BFT protocols.

**Chained BFT protocols.** Beyond CHS, 2CHS, and FHS mentioned above, there are other variants of chained BFT protocols. For instance, Streamlet [8] simplifies protocol design with different consensus rules; Jolteon [37] and Diem-BFT\_v4 [38] employ a quadratic view change mechanism, enabling two-phase block commitment under steady state; Wendy [39] leverages no-commit proofs to achieve optimal latency and linear message complexity; Marlin [19] introduces a ranking system and virtual blocks to counter forking attacks and reduce latency and bandwidth consumption. Despite differences in implementation details, these variants maintain the consensus paradigm of chained BFT. Thus, our framework may be extended to study these protocols.

**Performance analysis of chained BFT protocols.** Prior benchmarks [21]–[24], [27] focus on evaluating the throughput and latency metrics of various BFT protocols under different experimental settings. However, most of them do not consider the impact of attacks. Besides, the accuracy of evaluation results is affected by many factors such as implementation and deployment environment. Few studies analyze the performance of CHS protocols under attacks. Niu et al. [25] propose delay attack and forking attack, and provide theoretical analysis. Cohen et al. [26] design an attack and quantify its impact on throughput and latency through experiments. However, these studies only focus on a single protocol and cannot be directly adapted to analyze other protocols.

**MDP modeling of blockchain consensus.** There have been extensive studies [28]–[31], [40], [41] that apply MDP to evaluate the security and/or performance of blockchain consensus protocols. However, they focus on Nakamoto-style consensus, e.g., Bitcoin [2], Bitcoin-NG [42], or Ethereum [3]. Their models cannot be directly applied to analyze chained BFT protocols that follow significantly different design principles from Nakamoto-style consensus.

### III. SYSTEM MODEL AND METRICS

#### A. System Model

We consider a system with  $f$  Byzantine nodes among  $n$  ( $n \geq 3f + 1$ ) nodes by following existing chained BFT protocols [6], [7], [9], [10], [43]. The Byzantine nodes can behave arbitrarily, while honest nodes always follow the consensus rules. We define  $\alpha = f/n$  as the fraction of Byzantine nodes, with the remaining  $1 - \alpha$  representing the fraction of honest nodes. We assume a leader election mechanism in which the probability of electing a Byzantine leader is  $\alpha$ , with honest and Byzantine leaders proposing honest and adversarial blocks, respectively. We consider the worst-case situation where a single adversary controls all Byzantine nodes. The adversary attempts to degrade system performance (*i.e.*, minimizing the chain growth and commitment rate introduced shortly) with optimal strategies.

**Network model.** We assume a partially synchronous model by following previous work [23]–[25], [27], ensuring all honest nodes are in sync with the protocol’s state after Global Stabilization Time (GST). In particular, after GST, a message is guaranteed to be delivered within a known and bounded delay  $\Delta$ . This paper focuses on analyzing chained BFT protocols during network synchrony (*i.e.*, after GST) as prior analysis or evaluation works [23]–[25], [27]. We argue that during network asynchrony (*i.e.*, before GST), the adversary can cause more damage to the performance by utilizing network partitions, however, our analysis during network synchrony already reveals many insights about the design.

To show the impact of responsiveness, we assume the actual network delay between two nodes is  $\delta$  by following prior work [7], [44]–[46]. This delay varies depending on the real-time network conditions. We assume a fixed  $\delta$  in the analysis, while considering varied  $\delta$  in our experiments. We use  $k$  to denote the ratio between the maximum bound delay  $\Delta$  and the actual network delay  $\delta$ , *i.e.*,  $k = \Delta/\delta$ .

#### B. Evaluation Metrics

To evaluate the performance of chained BFT protocols, we introduce two metrics, *i.e.*, chain growth and commitment rate, as introduced below.

1) *Chain growth:* The chain growth  $G(\alpha)$  is defined as the rate of honest blocks appended to the main chain, given that the adversary corrupts a fraction  $\alpha$  of the total nodes. It indicates the impact of the adversary on system efficiency; the adversary can strategically minimize chain growth to reduce the system capacity for processing clients’ transactions, leading to significant service delays or system congestion.

Thus, we capture this by minimizing chain growth calculated in  $m$  views. We use  $B_{hi}$  and  $T_i$  to denote the number of honest blocks added to the main chain in the  $i$ -th view and time units consumed in the  $i$ -th view, respectively. We have:

$$G(\alpha) = \lim_{m \rightarrow \infty} \frac{\sum_{i=1}^m B_{hi}}{\sum_{i=1}^m T_i} \quad (1)$$

This metric considers only honest blocks, since adversarial leaders can selectively exclude honest clients’ transactions. Thus, it can reflect the *effective* capacity of processing transactions. To lower chain growth, the adversary can either prevent honest blocks from being included in the main chain or delay block generation. This metric is first proposed in [25], [27] to evaluate the performance of CHS.

2) *Commitment rate:* The commitment rate  $R(\alpha)$  is defined as the rate of block commitment event at the main chain, given the fraction of adversarial nodes  $\alpha$ . This metric captures system stability to continuously commit blocks and then confirm clients’ transactions. The adversary may target to minimize this metric to delay transaction confirmation, increasing transaction delay to affect time-sensitive applications. We denote whether blocks are committed in the  $i$ -th view by  $C_i$ , which is assigned the value of 1 if a commitment occurs in the  $i$ -th view, and 0 otherwise. Here, in chained BFT protocols, when a block is committed, all its uncommitted ancestor blocks are also committed. Thus, in a commitment event, several blocks may be committed. We have:

$$R(\alpha) = \lim_{m \rightarrow \infty} \frac{\sum_{i=1}^m C_i}{\sum_{i=1}^m T_i} \quad (2)$$

In chained BFT protocols, a block has to satisfy the commitment conditions to be committed (see Sec.II-A). Thus, the adversary deviates from the protocol to ruin the conditions. Note that this metric can also serve as an indicator of *liveness*. For example, if  $R(\alpha)$  is 0 for a chained BFT protocol, it means no transactions can be committed, *i.e.*, no liveness.

*Discussion.* Compared to commonly used throughput and latency metrics [21]–[24], these two metrics reflect performance under attacks more directly and are easier to trace in MDP modeling (introduced shortly). First, given the maximum batch size of transactions included in a block, chain growth directly reflects the maximum capacity of transactions included in honest nodes’ blocks, *i.e.*, the *effective* throughput. Meanwhile, commitment rate measures the frequency of block commitment, which is directly related to the time it takes for transactions to be confirmed, *i.e.*, latency. Second, two metrics focus on the block level, whereas throughput and latency reflect system performance at the transaction level. Ignoring unnecessary details makes them more traceable for analyzing strategies and state transitions in MDP modeling.

### IV. MDP MODELING

In this section, we use MDP to model three chained BFT protocols, *i.e.*, 2CHS, CHS, FHS, to show the impact of responsiveness on chain growth and commitment rate. We choose to model these three protocols as i) they achieve distinct responsiveness guarantees, and evaluating them will reveal insights on responsiveness, and ii) they are classic

protocols that inspire subsequent protocols and have been successfully integrated into practical blockchain platforms [17], [47], [48]. A detailed description of these three protocols is provided in §II-A.

### A. Overview

The Markov Decision Process (MDP) is a powerful mathematical framework for formalizing the decision-making process of an agent within a given environment. MDP captures the randomness in the agent’s decision-making and correlates the rewards it receives with the current state of the environment [49], [50]. MDP provides a way of representing actions taken in a sequence of states, where each state transition is associated with reward allocations. It enables us to find optimal attack strategies that may uncover vulnerabilities within each protocol. Furthermore, we can understand and defend against these found attacks. The framework models the consensus process and potential attacks across several chained BFT protocol designs, also enabling a comparison between them.

The MDP modeling includes four fundamental components:  $\langle S, A, P, R \rangle$ . In the context of chained BFT protocols,  $S$  is a set of all possible states that denote the current status of the chaining blocks and affect the decision-making process.  $A$  is the set of all possible actions that can be taken by the agent, *i.e.*, the adversary. The actions alter the state of the chaining blocks and determine the corresponding rewards.  $P$  corresponds to the transition probability function, which represents the likelihood of moving from one state to another based on the action.  $R$  reflects the benefits or penalties incurred by the system as a result of the transition. The reward is not the incentives obtained by nodes participating in consensus, but rather the reward of terms in calculating the metrics. The reward is essential in guiding the policy search toward actions that yield the most favorable outcomes.

Modeling chained BFT protocols (*i.e.*, state and action space) presents several challenges. First, it demands an accurate abstraction of the protocol, stripping away irrelevant details that do not influence the two metrics while accounting for all possible malicious behaviors. Second, the size of the state and action spaces must be carefully managed to ensure the model remains computationally solvable. Finally, the MDP model must be flexible enough to accommodate multiple chained BFT protocols, further complicating its design. In the following, we describe how moderate simplifications enable the development of a general MDP model for chained BFT protocols without compromising metric accuracy.

### B. Modeling Chained BFT Protocols

In this section, we introduce the MDP modeling of three chained BFT protocols. Due to space constraints, we take CHS as an example to illustrate the modeling process and only describe the differences in the modeling of other protocols.

1) *CHS*: CHS is the first chained BFT protocol that introduces responsiveness to accelerate the consensus process. Specifically, it introduces one extra phase to the consensus process. The introduced delay of the additional phase is considered insignificant compared to the time saved in view

change due to the responsiveness property, as claimed by authors in [7].

**State space.** The state space is a four-tuple form  $(\text{cS}, l_a, l_h, L)$ , as introduced below.

- **Commitment state (cS).** The  $\text{cS}$  represents the consecutive block structure that has already been formed. It is crucial because it directly affects the commitment of blocks. It has five possible values:  $\{0, 1, 2, 3, 3'\}$ . This is because CHS specifies that when three consecutive blocks are formed, the next block triggers a commitment. Therefore,  $\text{cS}$  is at most 3. The special value  $3'$  is used when three consecutive blocks are not continuous with the next block. In this case, the generation of the next block still triggers a commitment, but the value of  $\text{cS}$  will reset and become 1.
- **Uncommitted honest block ( $l_h$ ).** The notation  $l_h$  represents the number of honest blocks that have not been committed. It has three possible values:  $\{0, 1, 2\}$ . CHS locks the grandparent of the latest block, in the sense that the grandparent block and its prefix can be committed. Therefore, at most two blocks can be manipulated.
- **Uncommitted adversarial block ( $l_a$ ).** The notation  $l_a$  represents the number of adversarial blocks that have not been committed. It has two possible values:  $\{0, 1\}$ . The adversary can decide when honest nodes will see a block by releasing or temporarily hiding its block. Since honest nodes follow the consensus rule, once the adversary releases a certified adversarial block, it will not be overridden and can be considered as ultimately committed.
- **Current leader ( $L$ ).** The notation  $L$  represents the leader type (honest or adversarial) of the current view. It can be either honest (denoted as  $H$ ) or adversarial (denoted as  $A$ ).

**Actions.** The adversary can deviate from the prescribed consensus rules to maximize their benefits. The following actions defined in the MDP framework are available to the adversary.

- **Adopt.** The adversary adopts all available honest blocks that are not locked and discards the hidden adversarial blocks. If the adversary is the leader, it will propose a new block that extends the last adopted block. If the adversary is not the leader, it waits for an honest leader to propose a new block.
- **Wait.** If the adversary is elected as the leader, it will create a forking block or extend its prior forking block, to override honest blocks. Otherwise, it will wait for the honest leader to propose a new block.
- **Release.** This action is only available when there is a hidden adversarial block. After releasing the block at the beginning of the view, the leader will propose a new block to extend it. If the hidden block is a forking block, the non-locked honest blocks will be overridden.
- **Silent.** The adversary remains inactive in this view. If the adversary is the leader, it either proposes no block or an invalid one. If the leader is honest, the silence of the adversary does not affect the protocol, and honest nodes continue to vote for the block proposed in this view.

**State transition.** Table II presents a comprehensive view of all

Table II: State transition and reward matrices for CHS. The reward of  $B_h$  and  $C$  is analyzed in §IV-B.

State × Action	Resulting State	Pr.	T
(cS, 0, $l_h$ , H) Adopt	(min(cS+1, 3), 0, 1, A) (min(cS+1, 3), 0, 1, H)	$\alpha$ $1-\alpha$	$\delta+2\Delta$ $3\delta$
(cS, 1, $l_h$ , H) Adopt	(1, 0, 1, A) (1, 0, 1, H)	$\alpha$ $1-\alpha$	$\delta+2\Delta$ $3\delta$
(cS, 0, $l_h$ , A) Adopt	(cS, 1, 0, A) (cS, 1, 0, H)	$\alpha$ $1-\alpha$	$3\Delta$ $\delta+2\Delta$
(cS, 1, $l_h$ , A) Adopt	(0/3', 1, 0, A) (0/3', 1, 0, H)	$\alpha$ $1-\alpha$	$3\Delta$ $\delta+2\Delta$
(cS, 0, $l_h$ , H) Wait, Silent	(min(cS+1, 3), 0, min( $l_h$ +1, 2), A) (min(cS+1, 3), 0, min( $l_h$ +1, 2), H)	$\alpha$ $1-\alpha$	$\delta+2\Delta$ $3\delta$
(cS, 1, $l_h$ , H) Wait, Silent	(1, 0, min( $l_h$ +1, 2), A) (1, 0, min( $l_h$ +1, 2), H)	$\alpha$ $1-\alpha$	$\delta+2\Delta$ $3\delta$
(cS, 0, $l_h$ , A) Wait	(0/3', 1, $l_h$ , A) (0/3', 1, $l_h$ , H)	$\alpha$ $1-\alpha$	$3\Delta$ $\delta+2\Delta$
(cS, 1, 0, A) Wait	(min(cS+1, 3), 1, 0, A) (min(cS+1, 3), 1, 0, H)	$\alpha$ $1-\alpha$	$3\Delta$ $\delta+2\Delta$
(cS, 1, $l_h$ , A) $l_h > 0$ , Wait	(1, 1, 0, A) (1, 1, 0, H)	$\alpha$ $1-\alpha$	$3\Delta$ $\delta+2\Delta$
(cS, 1, 0, H) Release	(min(cS+2, 3), 0, 1, A) (min(cS+2, 3), 0, 1, H)	$\alpha$ $1-\alpha$	$\delta+2\Delta$ $3\delta$
(cS, 1, $l_h$ , H) $l_h > 0$ , Release	(2, 0, 1, A) (2, 0, 1, H)	$\alpha$ $1-\alpha$	$\delta+2\Delta$ $3\delta$
(cS, 1, 0, A) Release	(min(cS+1, 3), 1, 0, A) (min(cS+1, 3), 1, 0, H)	$\alpha$ $1-\alpha$	$3\Delta$ $\delta+2\Delta$
(cS, 1, $l_h$ , A) $l_h > 0$ , Release	(1, 1, 0, A) (1, 1, 0, H)	$\alpha$ $1-\alpha$	$3\Delta$ $\delta+2\Delta$
(cS, 0, $l_h$ , A) <sup>a</sup> Silent	(0, 0, $l_h-1$ , A) (0, 0, $l_h-1$ , H)	$\alpha$ $1-\alpha$	$2\Delta$ $\delta+\Delta$
(cS, $l_a$ , $l_h$ , A) <sup>b</sup> Silent	(0, 0, $l_h$ , A) (0, 0, $l_h$ , H)	$\alpha$ $1-\alpha$	$2\Delta$ $\delta+\Delta$

<sup>a</sup>  $l_h > 0 \wedge cS \neq 0/3'$

<sup>b</sup>  $l_a = 1 \vee (l_a = 0 \wedge (l_h = 0 \vee (l_h > 0 \wedge cS = 0/3')))$

possible state transitions under each possible state, and derives each state transition, including its probability, reward and the resulting state.

- **Commitment state (cS).** When the leader is honest, the transition of cS mainly depends on  $l_a$ . If  $l_a=0$ , it means that there is no hidden adversarial block, and the actions Adopt, Wait and Silent taken by the adversary increase cS by 1. If  $l_a > 0$ , these actions signify that the adversary abandons its block. This breaks the consecutive structure and cS resets to 0. However, with the honest leader proposing a new block, cS increases to 1. When the adversary chooses Release with  $l_h > 0$ , it means the released block is a forking block. This again breaks the consecutive structure, and the released block together with the new proposed honest block make cS to 2. If  $l_h=0$ , cS increases by 2.

When the leader is adversarial, the transition can be categorized based on the action taken by the adversary. If an Adopt action is taken and  $l_a=0$ , the adversary will extend the previous honest block, and the consecutive structure will be preserved. Also, as the proposed adversarial block is temporarily hidden, cS remains unchanged. When  $l_a > 0$ , the adversary takes Adopt action to give up the hidden

block, and the consecutive structure is destroyed, and thus cS is reset. If the previous cS equals 3, then cS becomes 3', otherwise cS becomes 0. For Wait and Release actions, if a fork is formed, cS will be reset; If the previous adversarial block is extended, cS increases by 1. If the Silent action is taken, cS becomes 0.

- **Uncommitted adversarial block ( $l_a$ ).** If the current leader is adversarial and takes Adopt, Wait, or Release actions, it will propose a temporarily hidden adversarial block, and  $l_a$  becomes 1. In all other cases,  $l_a$  becomes 0.
- **Uncommitted honest block ( $l_h$ ).** The adversary's actions of Adopt and Release will cause  $l_h$  to become 0, and  $l_h$  will increase by 1 if the current leader is honest, otherwise it will remain unchanged. In the Wait action, if the adversary extends its block, the hidden block will be passively released, and  $l_h$  will increase by 1 if the current leader is honest, otherwise it will remain unchanged. In Silent action, if the leader is honest,  $l_h$  will increase by 1. If the leader is adversarial and an honest block is generated in the previous view, the block will be excluded and  $l_h$  will be reduced by 1.
- **Current Leader ( $L$ ).** There are two possible transitions of  $L$  upon each action: being adversarial with a probability of  $\alpha$ , and being honest with  $1-\alpha$ .

**Reward allocation.** Rewards are allocated in each state transition to certain variables used to calculate the chain growth and commitment rate. The two metrics are calculated from the number of honest blocks in the chain ( $B_h$ ), the commitment times ( $C$ ), and the time consumed in the process ( $T$ ). Due to space constraints, we only show the common variable  $T$  used in the two metrics in Table II.

- **Committed honest block ( $B_h$ ).**  $B_h$  will increase by 1 if an honest block is eventually committed on the chain. After the adversary takes Adopt action, the existing honest blocks will be accepted by the adversary, preventing them from being overridden, and  $B_h$  will increase by  $l_h$ . In addition,  $B_h$  will increase by 1 when  $l_h$  transits to  $l_h+1$  if  $l_h=2$ . Due to the locking rule, if  $l_h=2$ , the subsequent block will cause its grandparent block to be locked, and  $B_h$  will also increase by 1.
- **Commitment times ( $C$ ).**  $C$  increases by 1 for each block commitment. In CHS, when a new block extends three consecutive blocks, it triggers a commitment. This requires cS to be 3 or 3', and meets one of the following three conditions: 1) the current leader is honest and the adversary takes Adopt, Wait, or Silent actions; 2) The current leader is honest, and the adversary takes Release action without any forks ( $l_h=0$ ); or 3) The current leader is adversarial and takes Wait or Release actions without a fork ( $l_h=0$ ).
- **Elapsed time ( $T$ ).** Recall that we use  $\delta$  and  $\Delta$  to denote the actual network delay and upper bound network delay after GST, respectively. The time consumed within each view consists of three parts: 1) the leader broadcasts a block, 2) the next leader collects votes from other nodes, and 3) the view-change process.

For the first two parts, they take  $\delta$  if the leader is honest, and  $\Delta$  otherwise. For the last one, it is determined by the next leader and the responsiveness/non-responsiveness properties of the protocol. Due to the responsiveness of CHS, the view-change process takes  $\delta$  if the leader is honest and  $\Delta$  otherwise. The leader of two consecutive views can be divided into four groups, and their consumption time differs. Note that if an adversarial leader takes the `Silent` action, honest nodes will trigger timeout upon the leader proposing the block (part 1) and directly entering the view change (part 3) without collecting votes (part 2).

2) *2CHS*: 2CHS shares a similar design as CHS and Casper [6], and can also be viewed as the pipelined version of Tendermint [5]. As mentioned previously, 2CHS has one less phase than CHS, but does not have responsiveness. Besides, the commitment of 2CHS slightly differs from CHS. In 2CHS, the first block of two consecutive blocks and its previous blocks will be committed if a new block extends the second block. In other words, in 2CHS, the parent block of a certified block, instead of the grandparent block, is locked.

We enumerate the state transition and reward matrices for 2CHS in Table III. The state space of 2CHS has the same four-tuple as CHS. Due to the two consecutive blocks structure,  $l_h$  is at most 1, and  $cS$  can be  $\{0, 1, 2, 2'\}$ . This also leads to corresponding changes in the state transition and reward allocation of  $B_h$  and  $C$ . When  $l_h$  increases from 1 to  $l_h+1$ ,  $B_h$  will increase by 1. When  $cS$  becomes 2 or  $2'$ , honest nodes trigger a commitment, and  $C$  increases by 1. For time consumption, the rewards for  $T$  in the leader-based stage remain unchanged, but since 2CHS is not responsive, the view change part always takes  $\Delta$  time regardless of the identity of the next leader.

3) *FHS*: FHS is a responsive two-phase chained BFT protocol, which allows a leader to include  $f+1$  latest QCs in its block. Compared with CHS, the QC inclusion in FHS slightly increases the message exchange overhead, but does not require an additional phase to achieve responsiveness. Despite FHS's resilience against forking attacks, honest nodes may still lose blocks. This is because votes sent to a subsequent adversarial leader could be hidden, preventing the formation of a QC. As a result, the actions available to the adversary in FHS are the same as 2CHS.

The state transition and reward allocation of FHS are the same as 2CHS, except for  $T$ . Besides responsiveness, FHS optimizes the view change process by incorporating the "happy path" mechanism, where the next leader skips the view change if they successfully form the QC of the previous block. This QC is ensured to be the highest QC, so honest nodes can directly propose a new block based on this QC. This mechanism further reduces  $T$ .

## V. THEORETICAL RESULTS

In this section, we obtain the performance results of three chained BFT protocols based on our MDP model. By observing these results, we aim to answer a key question: *How do the responsiveness property and different responsiveness designs affect the chain growth and commitment rate of chained BFT protocols?*

Table III: State transition and reward matrices for 2CHS. The reward of  $B_h$  and  $C$  is analyzed in §IV-B.

State $\times$ Action	Resulting State	Pr.	T
$(cS, 0, l_h, H)$ Adopt	$(\min(cS+1, 2), 0, 1, A)$ $(\min(cS+1, 2), 0, 1, H)$	$\alpha$ $1-\alpha$	$\delta+2\Delta$ $2\delta+\Delta$
$(cS, 1, l_h, H)$ Adopt	$(1, 0, 1, A)$ $(1, 0, 1, H)$	$\alpha$ $1-\alpha$	$\delta+2\Delta$ $2\delta+\Delta$
$(cS, 0, l_h, A)$ Adopt	$(cS, 1, 0, A)$ $(cS, 1, 0, H)$	$\alpha$ $1-\alpha$	$3\Delta$ $3\Delta$
$(cS, 1, l_h, A)$ Adopt	$(0/2', 1, 0, A)$ $(0/2', 1, 0, H)$	$\alpha$ $1-\alpha$	$3\Delta$ $3\Delta$
$(cS, 0, l_h, H)$ Wait, Silent	$(\min(cS+1, 2), 0, \min(l_h+1, 1), A)$ $(\min(cS+1, 2), 0, \min(l_h+1, 1), H)$	$\alpha$ $1-\alpha$	$\delta+2\Delta$ $2\delta+\Delta$
$(cS, 1, l_h, H)$ Wait, Silent	$(1, 0, \min(l_h+1, 1), A)$ $(1, 0, \min(l_h+1, 1), H)$	$\alpha$ $1-\alpha$	$\delta+2\Delta$ $2\delta+\Delta$
$(cS, 0, l_h, A)$ Wait	$(0/2', 1, l_h, A)$ $(0/2', 1, l_h, H)$	$\alpha$ $1-\alpha$	$3\Delta$ $3\Delta$
$(cS, 1, 0, A)$ Wait	$(\min(cS+1, 2), 1, 0, A)$ $(\min(cS+1, 2), 1, 0, H)$	$\alpha$ $1-\alpha$	$3\Delta$ $3\Delta$
$(cS, 1, l_h, A)$ $l_h > 0$ , Wait	$(1, 1, 0, A)$ $(1, 1, 0, H)$	$\alpha$ $1-\alpha$	$3\Delta$ $3\Delta$
$(cS, 1, l_h, H)$ Release	$(2, 0, 1, A)$ $(2, 0, 1, H)$	$\alpha$ $1-\alpha$	$\delta+2\Delta$ $2\delta+\Delta$
$(cS, 1, 0, A)$ Release	$(\min(cS+1, 2), 1, 0, A)$ $(\min(cS+1, 2), 1, 0, H)$	$\alpha$ $1-\alpha$	$3\Delta$ $3\Delta$
$(cS, 1, l_h, A)$ $l_h > 0$ , Release	$(1, 1, 0, A)$ $(1, 1, 0, H)$	$\alpha$ $1-\alpha$	$3\Delta$ $3\Delta$
$(cS, 0, l_h, A)^a$ Silent	$(0, 0, l_h-1, A)$ $(0, 0, l_h-1, H)$	$\alpha$ $1-\alpha$	$2\Delta$ $2\Delta$
$(cS, l_a, l_h, A)^b$ Silent	$(0, 0, l_h, A)$ $(0, 0, l_h, H)$	$\alpha$ $1-\alpha$	$2\Delta$ $2\Delta$

<sup>a</sup>  $l_h > 0 \wedge cS \neq 0/2'$

<sup>b</sup>  $l_a = 1 \vee (l_a = 0 \wedge (l_h = 0 \vee (l_h > 0 \wedge cS = 0/2')))$

To obtain the results, we cannot directly apply our metrics to traditional MDP techniques, because the objective functions are non-linear, and the adversary aims to minimize them. Therefore, we first refer to the procedure developed by Sapirshstein et al. [28] to linearize the objective functions. Taking  $G'(\alpha)$  as an example, we first define a new objective function  $G'(\alpha)$ :

$$G'(\alpha) = 1 - \mathbb{E} \left[ \liminf_{m \rightarrow \infty} \frac{\sum_{i=1}^m B_{hi}}{\sum_{i=1}^m T_i} \right]. \quad (3)$$

The adversary's goal is to maximize  $G'(\alpha)$ . We use  $\rho$  to denote the value of  $G'(\alpha)$ , and define a transformation function  $w_\rho: \mathbb{N}^2 \rightarrow \mathbb{R}$  as:

$$w_\rho(B_h, T) = (1 - \rho)T - B_h, \quad (4)$$

where  $B_h$  and  $T$  are the reward of the honest nodes and the time consuming in consensus process, respectively. The reward matrix of the MDP model is determined by  $w_\rho$ . Suppose that  $v_\rho^\pi$  represents the expected value under policy  $\pi$ , then

$$v_\rho^\pi = \mathbb{E} \left[ \liminf_{m \rightarrow \infty} \frac{1}{m} \sum_{i=1}^m w_\rho(B_{hi}(\pi), T_i(\pi)) \right]. \quad (5)$$

Let  $v_\rho^*$  denotes the expected value under the optimal policy, i.e.,  $v_\rho^* = \max_\pi \{v_\rho^\pi\}$ . According to [28], if there exists some  $\rho$  satisfies  $v_\rho^* = 0$ , then the policy also maximizes  $G'(\alpha)$ .

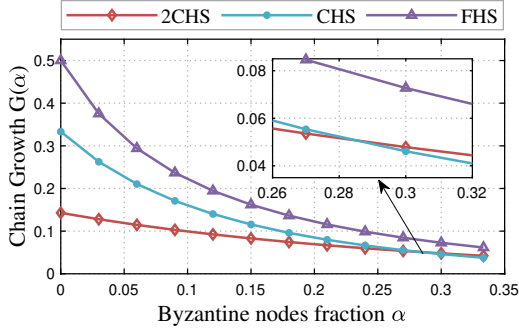


Figure 3: The chain growth of 2CHS, CHS, and FHS.

Given that  $v_0^* > 0$  and  $v_1^* < 0$ , and  $v_\rho^*$  is monotonically decreasing in  $\rho \in [0, 1]$ , we can apply the binary search algorithm in [28] to find  $\rho$  for  $v_\rho^* = 0$ , denoted as  $\bar{\rho}$ . This  $\bar{\rho}$  represents the maximum possible value of  $G'(\alpha)$ , which implies  $1 - \bar{\rho}$  is the minimum possible value of  $G(\alpha)$ . The minimum value of  $R(\alpha)$  can be derived in the same manner.

The range of  $\alpha$  is from 0 to  $1/3$ , not including  $1/3$  itself (the system's maximum tolerable Byzantine nodes), with  $\alpha$  increasing by 0.03 at each step, and a precision of  $10^{-4}$ . We assume that the maximum network delay  $\Delta$  and the actual delay  $\delta$  satisfy the relationship  $\Delta = 5\delta$ . We obtain the theoretical optimal values and attack strategies through the framework, and then compare our results with existing attack strategies. The MDP source code is provided in [33].

#### A. Theoretical Results Analysis

We consider the chain growth and commitment rate of the protocols under optimal attack strategies found by the MDP model. Fig. 3 and Fig. 4 provide the evaluation results of chain growth and commitment rate, respectively.

**The performance under attacks.** There is a downward trend in both of chain growth and commitment rate of the three protocols as  $\alpha$  grows. Fig. 3 shows that, when the fraction  $\alpha$  of Byzantine nodes increases from 0 to 0.3, the chain growth of CHS decreases from 0.333 to 0.046, and chain growth of FHS decreases from 0.5 to 0.073. For 2CHS, the chain growth drops to nearly one-third when  $\alpha$  is close to 0.3. Fig. 4 shows that as  $\alpha$  increases from 0 to  $1/3$ , the commitment rate of CHS drops from 0.333 to 0.027, FHS drops from 0.5 to 0.042, and 2CHS decreases from 0.143 to 0.03. This is because when  $\alpha$  increases, more adversarial nodes are elected as leaders, and adversarial leaders can attack the two performance metrics.

**The impact of responsiveness.** For CHS and FHS with responsiveness, chain growth and commitment rate are decreased significantly with smaller  $\alpha$ . For example, in FHS, when  $\alpha$  increases from 0 to 0.2, the chain growth decreases by 31%; and when  $\alpha$  increases from 0.2 to  $1/3$ , chain growth decreases by 13%. In addition, with larger  $\alpha$ , responsiveness brings less benefits to performance: responsive CHS and FHS achieve comparable chain growth and commitment rate with non-responsive 2CHS when  $\alpha$  reaches  $1/3$ . When  $\alpha$  is small, the impact of the adversary's attacks is limited, and the responsiveness property can effectively accelerate the view

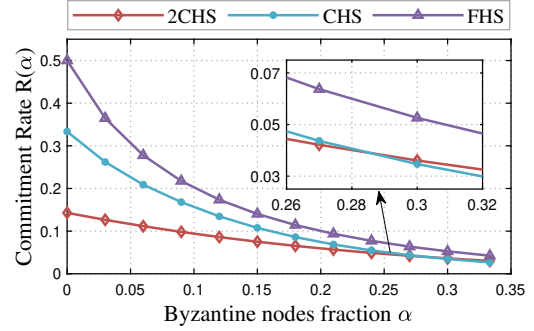


Figure 4: The commitment rate of 2CHS, CHS, and FHS.

change. So the impact of responsiveness on performance is relatively large when  $\alpha$  is small, but as  $\alpha$  increases, its advantage gradually weakens.

**Comparison between responsive and non-responsive protocols.** We observe that FHS outperforms the other two protocols, and the non-responsive 2CHS lags behind in most cases. When  $\alpha = 0$ , the chain growth of FHS is 3.5 and 1.5 times compared to 2CHS and CHS, respectively. When  $\alpha = 1/3$ , the chain growth of FHS becomes 1.5 and 1.6 times compared to 2CHS and CHS. When  $\alpha = 0.3$ , the commitment rate of FHS becomes 1.5 times compared to 2CHS and CHS.

It is noteworthy that the evaluation lines of 2CHS and CHS intersect between  $\alpha = 0.27$  and  $\alpha = 0.3$ . After the intersection, 2CHS performs better than CHS. This is because of the committing rule of three consecutive blocks in CHS. For chain growth, the additional phase allows the adversary to override two honest blocks in a forking attack. For commitment rate, triggering a block commitment is less likely compared to the rule of two consecutive blocks, especially with larger  $\alpha$ . This indicates that in some cases, implementing responsiveness by adding a new phase may not necessarily improve the performance of the protocol. This is also evidenced in FHS that achieves better chain growth and commitment rate due to its optimization for the happy paths.

**Considerations for Protocol Design** The extra communication phase in CHS and the latest QC proof in FHS, while enhancing responsiveness, also increase message overhead and processing time. This can exacerbate transmission delays and the risk of network congestion, particularly impacting nodes with limited resources by slowing their message processing and consensus participation. In networks with a higher fraction of Byzantine nodes, these negative effects of responsiveness become more pronounced. Therefore, when implementing responsiveness in protocol design, it is crucial to consider its benefits against potential drawbacks, especially in networks with Byzantine nodes.

**Summary.** The evaluation shows that attacks can significantly degrade chain growth and commitment rate, especially when the fraction  $\alpha$  is large. Furthermore, achieving responsiveness can improve chain growth and commitment rate when  $\alpha$  is small. However, when  $\alpha$  is relatively large, responsiveness brings less benefit to both metrics. It indicates that although responsiveness is an important property, certain designs for



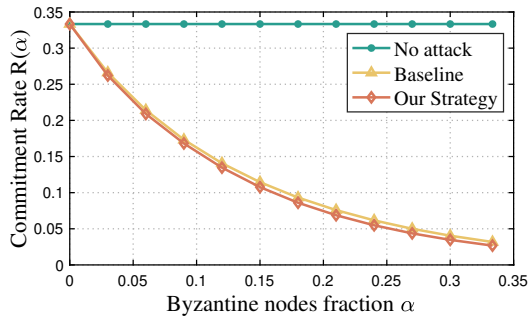


Figure 5: The commitment rate of CHS under our strategy, the baseline (simple strategy) and without attack.

achieving responsiveness may not necessarily improve protocol performance in all cases. Appropriate implementation needs to be considered based on protocol needs, especially in the presence of attacks.

### B. Comparison to Existing Attack Strategies

Modeling chained BFT protocols as MDPs allows us to derive optimal adversarial strategies and evaluate the corresponding worst-case performance metrics. To demonstrate the effectiveness of our approach, we compare our strategies against the baseline strategy in [20], [27]. Using this strategy, adversarial leaders remain silent during their views, forcing a timeout in the proposal phase and triggering a view change for all nodes. This behavior resets the consecutive block count, effectively preventing block commitments and degrading system performance.

Fig. 5 illustrates the commitment rate of CHS under different attack strategies. Both the simple attack strategy and our proposed strategy result in a significant reduction in commitment rate compared to scenarios without attacks. Notably, the impact becomes more pronounced as  $\alpha$  increases. For instance, when  $\alpha = 0.3$ , commitment rate under the simple attack strategy and our strategy drops to 12% and 10%, respectively, of the commitment rate without attacks.

Our strategy consistently outperforms the simple attack approach by guiding the adversary to take optimal actions in specific scenarios, particularly in corner cases. For example, when an adversarial node is elected as the leader, and no three-consecutive block structure exists, the adversary can propose a block but selectively send the proposal to a subset of honest nodes. This tactic prevents honest nodes from gathering enough votes to form a QC while also avoiding a timeout in the proposal phase. Consequently, the adversary resets the number of consecutive blocks while extending the consumed time. This sophisticated approach amplifies the attack’s impact on commitment rate by leveraging the protocol’s inherent vulnerabilities. Since the case shows with small probability, the performance gap between the baseline and our strategy remains moderate. Nevertheless, the powerful MDP framework enables us to find the optimal strategy for more complex chained BFT protocols, advancing existing attack methods.

## VI. EXPERIMENTS

The theoretical models provide a foundation for understanding the impact of responsiveness on system performance under various conditions. To study the practical implications of the theoretical results, we implement the three studied chained BFT protocols and evaluate their chain growth and commitment rate in real-world scenarios. Besides, we consider more factors of practical systems such as fluctuating network delay in evaluation. The adversary in our experiments employs the attack strategies found by MDP in §V. The experiment will check whether the experimental results align with the theoretical results and examines the impact of fluctuating network delay  $\delta$  on the results.

### A. Implementation and Setup

**Implementation.** We have extended an open-source evaluation platform Bamboo [27] in the Go language to implement the chained BFT protocols. The source code can be found at [34]. Our modifications add approximately 1000 lines of code to Bamboo for implementing attack strategies on CHS, 2CHS, and FHS.

**System setup.** The experimental environment includes 4 servers, each equipped with a 16-core CPU, 32GB RAM with the operating system of Ubuntu Server 22.04. The network latency between servers is approximately 1ms. The experimental environment consists of a fixed number of nodes, with the flexibility to control the fraction of Byzantine nodes within the network. We set up a network topology that could accommodate up to 60 nodes (each server supports 15 nodes), with the capability to introduce up to 18 Byzantine nodes to test the system’s performance under attacks. The key parameters for the experiments include the fraction of Byzantine nodes and the network latency settings. To align with the theoretical setting, *i.e.*,  $\Delta = 5\delta$ , we first set the minimum delay between nodes at 100 ms and the maximum latency for communication at 500 ms. Meanwhile, to demonstrate the impact of a random network environment, we set the minimum delay between nodes to a fluctuating value between 25 ms and 50 ms, and conduct corresponding experiments based on the previous ones. The fluctuation of delay conforms to a uniform distribution. We run each experiment for 10 minutes and averaged the results over six independent runs.

### B. Chain Growth

We first use a fixed network delay  $\delta = 100ms$  in experiments. Fig. 6a shows that the experimental results closely match the results in §V. The chain growth of CHS, 2CHS and FHS gets worse as  $\alpha$  increases. When  $\alpha = 0.3$ , chain growth of 2CHS drops to 35% of that when  $\alpha = 0$ . FHS outperforms 2CHS and CHS in chain growth, and 2CHS and CHS have an intersection point.

In the presence of network delay fluctuations, as shown in Fig. 6b and Fig. 6c, we observe that the performance of chain growth remains largely consistent with the stable delay scenario. However, the measurement errors indicated by the error bars increase with the delay fluctuations. In the case

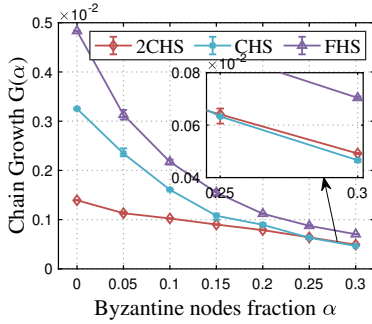
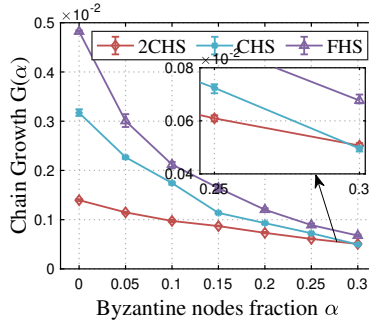
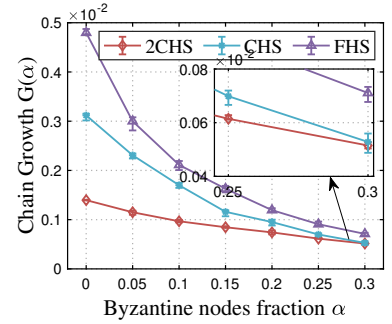
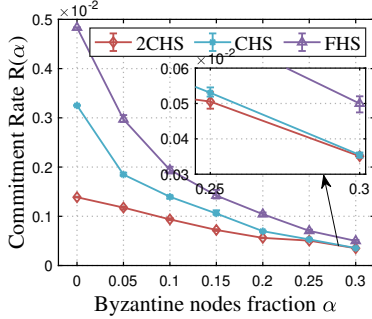
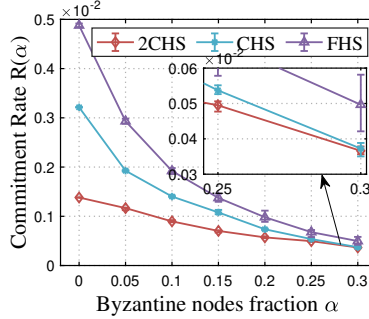
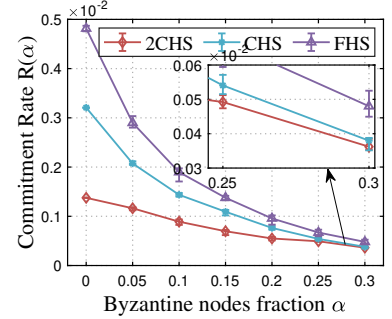
(a) Chain growth when  $\delta = 100ms$ .(b) Chain growth when  $\delta = 100 \pm 25ms$ .(c) Chain growth when  $\delta = 100 \pm 50ms$ .(d) Commitment rate when  $\delta = 100ms$ .(e) Commitment rate when  $\delta = 100 \pm 25ms$ .(f) Commitment rate when  $\delta = 100 \pm 50ms$ .

Figure 6: The experimental results of chain growth and commitment rate of 2CHS, CHS, and FHS with varying network delay  $\delta$ .

of CHS, with a fluctuation range of 25ms, the measurement error is 1.3 times compared to the stable delay, and with a fluctuation range of 50ms, the error doubles compared to without fluctuation. Overall, the experimental results of chain growth with stable delay are consistent with the theoretical results, thus confirming the findings in §V.

### C. Commitment Rate

Fig. 6d shows the commitment rate results under stable network delay. The commitment rate also shows a decline as  $\alpha$  grows, with FHS outperforming 2CHS and CHS. As  $\alpha$  increases from 0 to 0.3, commitment rate of FHS decreases by 11%. Fig. 6e and Fig. 6f show the evaluation results with a delay fluctuation amplitude of 25 and 50 ms. The commitment rate is similar to that with stable delay. The measurement errors increase with increasing fluctuations. Regarding 2CHS, at fluctuation ranges of 25ms and 50ms, the measurement errors are 1.2 times and 2.1 times compared to those without fluctuations, respectively. For FHS, the measurement errors become 2 and 2.3 times of the original values, respectively. CHS and FHS show more significant deviations compared to 2CHS. While the measurement error increases with more fluctuating network latency, the average evaluation results remain largely unchanged and the observed trend is consistent with previous experiments.

In a nutshell, the experiments provide direct evidence supporting the validity of the framework, and the results of chain growth and commitment rate from the framework remain robust even in realistic network settings.

## VII. DISCUSSION

We present some limitations to be addressed in future works.

**Considering more factors.** In order to analyze the worst-case scenario, we simplify the adversary's behaviors in the MDP modeling. For example, we assume the adversary coordinates all Byzantine nodes without network delay, which may not hold in dynamic and diverse network conditions. As a result, the system performance under attack scenarios may be over-estimated.

**Considering defense.** We notice that some latest BFT protocols consider accountability and forensics support [51], [52], in which honest nodes can detect certain attacks and identify Byzantine nodes. Thus, the attack may be mitigated due to the punishment. However, these defenses do not eliminate attacks, as attackers can still launch attacks if they operate within the punishment threshold or are indifferent to the penalties.

**Asynchronous evaluation.** Our analysis focuses on synchronous periods after GST, which means that message delivery between nodes is confined within a known bound. The attacks on protocol performance may be more severe in asynchronous situations due to network partitions. Therefore, modeling and evaluating chained BFT protocol in asynchronous periods (*i.e.*, before GST) may reveal more insights about the impact of responsiveness.

**Extending the framework.** We primarily select the classic protocols that have been deployed in real distributed systems and influence subsequent BFT protocols [53]–[55]. At the same time, there are also some new chained BFT protocols, such as Streamlet [8], Marlin [19], and BeeGees [20], that differ in design (see §II-B) from three protocols we analyzed.

Nevertheless, our modeling framework could be applied to these protocols with slight modifications because they share the same consensus paradigm. The methodology and analytical tools developed in this study can be extended to other protocols with minimal adjustments. For example, our framework is still applicable to Streamlet. Due to space constraints, we show our further analysis of Streamlet in Appendix A.

## VIII. CONCLUSION

In this paper, we analyze the performance of chained BFT protocols through a unified framework with two metrics, chain growth and commitment rate. This framework is constructed upon an MDP model, which allows us to evaluate the worst-case performance of three representative protocols (*i.e.*, CHS, 2CHS and FHS) under attacks. The evaluation reveals the effect of responsiveness, which is an important property in protocol design. The framework also provides the optimal attack strategies, discovering better strategies than previous work, which can further decrease commitment rate. We also conduct an experimental deployment and confirm that the experimental results of our metrics under optimal strategies on practical platforms align well with our theoretical results. In addition, the framework can be extended to other chained BFT protocols and provides a convenient tool for performance comparison among these protocols.

## REFERENCES

- [1] Y. Gilad, R. Hemo, S. Micali, G. Vlachos, and N. Zeldovich, "Algorand: Scaling Byzantine agreements for cryptocurrencies," in *SOSP*, 2017.
- [2] S. Nakamoto, "Bitcoin: A peer-to-peer electronic cash system," *Working Paper*, 2008.
- [3] G. Wood, "Ethereum: A secure decentralised generalised transaction ledger Byzantium version," *Ethereum project yellow paper*, 2018. [Online]. Available: <https://github.com/ethereum/yellowpaper>
- [4] D. Labs, "Crypto kitties," <https://www.cryptokitties.co/>.
- [5] E. Buchman, "Tendermint: Byzantine Fault Tolerance in the age of blockchains," *M.Sc. Thesis, University of Guelph, Canada*, Jun 2016.
- [6] V. Buterin and V. Griffith, "Casper the Friendly Finality Gadget," *CoRR*, vol. abs/1710.09437, 2017.
- [7] M. Yin, D. Malkhi, M. K. Reiter, G. G. Gueta, and I. Abraham, "HotStuff: BFT consensus with linearity and responsiveness," in *PODC*, 2019.
- [8] B. Y. Chan and E. Shi, "Streamlet: Textbook streamlined blockchains," *IACR Cryptol. ePrint Arch.*, 2020.
- [9] M. M. Jalalzai, J. Niu, C. Feng, and F. Gai, "Fast-HotStuff: A fast and robust BFT protocol for blockchains," *TDSC*, 2023.
- [10] D. Malkhi and K. Nayak, "HotStuff-2: Optimal two-phase responsive BFT," *Cryptology ePrint Archive*, 2023.
- [11] X. Lab, "XuperChain Platform," June 2021. [Online]. Available: <https://github.com/xuperchain/xuperchain>
- [12] "Introduction to Hyperchains," <https://blog.matter-labs.io/introduction-to-hyperchains-fdb33414ead7>, retrieved Nov, 2024.
- [13] C. Schwarz-Schilling, J. Neu, B. Monnot, A. Asgaonkar, E. N. Tas, and D. Tse, "Three attacks on Proof-of-Stake Ethereum," in *FC*, 2022.
- [14] "Aptos homepage," <https://aptoslabs.com>, retrieved Nov, 2024.
- [15] Y. Guo, Q. Yang, H. Zhou, W. Lu, and S. Zeng, "Syetem and methods for selection and utilizing a committee of validator nodes in a distributed system," Cypherium Blockchain, Feb 2020, patent. [Online]. Available: <https://github.com/cypherium/patent>
- [16] A. Hentschel, Y. Hassanzadeh-Nazarabadi, R. Seraj, D. Shirley, and L. Lafrance, "Flow: Separating consensus and compute-block formation and execution," *arXiv preprint arxiv:2002.07403*, 2002.
- [17] J. McKane, "EVM and the road to Zilliqa 2.0 - Upgrading network efficiency," <https://blog.zilliqa.com/evm-and-the-road-to-zilliqa-2-0-upgrading-network-efficiency/>, retrieved Nov, 2024.
- [18] "Revolution Proof of Stake," <https://revolution.deso.com/>, retrieved Nov, 2024.
- [19] X. Sui, S. Duan, and H. Zhang, "Marlin: Two-phase BFT with linearity," in *DSN*, 2022.
- [20] N. Giridharan, F. Suri-Payer, M. Ding, H. Howard, I. Abraham, and N. Crooks, "BeeGees: stayin' alive in chained BFT," in *PODC*, 2023.
- [21] T. T. A. Dinh, J. Wang, G. Chen, R. Liu, B. C. Ooi, and K.-L. Tan, "Blockbench: A framework for analyzing private blockchains," in *SIGMOD*, 2017.
- [22] G. Shapiro, C. Natoli, and V. Gramoli, "The performance of Byzantine Fault Tolerant blockchains," in *NCA*, 2020.
- [23] M. J. Amiri, C. Wu, D. Agrawal, A. El Abbadi, B. T. Loo, and M. Sadoghi, "The bedrock of Byzantine Fault Tolerance: A unified platform for BFT protocols analysis, implementation, and experimentation," in *NSDI*, 2024.
- [24] V. Gramoli, R. Guerraoui, A. Lebedev, C. Natoli, and G. Voron, "Diablo: A benchmark suite for blockchains," in *Eurosys*, 2023.
- [25] J. Niu, F. Gai, M. M. Jalalzai, and C. Feng, "On the performance of pipelined HotStuff," in *INFOCOM*, 2021.
- [26] S. Cohen, R. Gelashvili, L. K. Kogias, Z. Li, D. Malkhi, A. Sonnino, and A. Spiegelman, "Be aware of your leaders," in *FC*, 2022.
- [27] F. Gai, A. Farahbakhsh, J. Niu, C. Feng, I. Beschastnikh, and H. Duan, "Dissecting the performance of Chained-BFT," in *ICDCS*, 2021.
- [28] A. Sapirshstein, Y. Sompolinsky, and A. Zohar, "Optimal selfish mining strategies in Bitcoin," in *FC*, 2017.
- [29] A. Gervais, G. O. Karame, K. Wüst, V. Glykantzis, H. Ritzdorf, and S. Capkun, "On the security and performance of Proof of Work blockchains," in *CCS*, 2016.
- [30] R. Zhang and B. Preneel, "On the necessity of a prescribed block validity consensus: Analyzing Bitcoin unlimited mining protocol," in *CoNEXT*, 2017.
- [31] J. Niu, Z. Wang, F. Gai, and C. Feng, "Incentive analysis of Bitcoin-NG, revisited," *SIGMETRICS Perform. Eval. Rev.*, 2021.
- [32] "Bamboo: Evaluation framework of chained BFT," <https://github.com/gitferry/bamboo>, retrieved Nov, 2024.
- [33] "MDP source code," <https://github.com/anonymousust/framework/tree/main/MDPModel/>.
- [34] "Attack implementation based on Bamboo," <https://github.com/anonymousust/framework/tree/main/experiment>.
- [35] P.-L. Aublin, R. Guerraoui, N. Knežević, V. Quéma, and M. Vukolić, "The next 700 BFT protocols," *TOCS*, 2015.
- [36] D. Gupta, L. Perronne, and S. Bouchenak, "BFT-Bench: A framework to evaluate BFT protocols," in *ICPE*, 2016.
- [37] R. Gelashvili, L. Kokoris-Kogias, A. Sonnino, A. Spiegelman, and Z. Xiang, "Jolteon and Ditto: Network-adaptive efficient consensus with asynchronous fallback," in *FC*. Springer, 2022.
- [38] D. Team, "DiemBFT v4: State machine replication in the Diem blockchain," Technical Report. Diem. [https://developers.diem.com/papers/diem-consensus ...](https://developers.diem.com/papers/diem-consensus...), Tech. Rep., 2021.
- [39] N. Giridharan, H. Howard, I. Abraham, N. Crooks, and A. Tomescu, "No-commit proofs: Defeating livelock in bft," *Cryptology ePrint Archive*, 2021.
- [40] C. Feng and J. Niu, "Selfish mining in Ethereum," in *ICDCS*. IEEE, 2019.
- [41] R. Zhang and B. Preneel, "Lay down the common metrics: Evaluating Proof-of-Work consensus protocols' security," in *S&P*. IEEE, 2019.
- [42] I. Eyal, A. E. Gencer, E. G. Sirer, and R. Van Renesse, "Bitcoin-NG: A scalable blockchain protocol," in *NSDI*, 2016.
- [43] E. Shi, "Streamlined blockchains: A simple and elegant approach (a tutorial and survey)," in *Asiacrypt*, 2019.
- [44] I. Abraham, K. Nayak, and N. Shrestha, "Optimal good-case latency for rotating leader synchronous BFT," *Cryptology ePrint Archive*, 2021.
- [45] A. Momose, J. P. Cruz, and Y. Kaji, "Hybrid-BFT: Optimistically responsive synchronous consensus with optimal latency or resilience," *Cryptology ePrint Archive*, 2020.
- [46] I. Abraham, D. Malkhi, K. Nayak, L. Ren, and M. Yin, "Sync HotStuff: Simple and practical synchronous state machine replication," in *S&P*. IEEE, 2020.
- [47] D. Ryan and C.-C. Liang, "EIP 1011: Hybrid Casper FFG," ThunderCore, April 2018. [Online]. Available: <https://eips.ethereum.org/EIPS/eip-1011>
- [48] J. Kwon and E. Buchman, "Cosmos: A network of distributed ledgers," 2016.
- [49] O. Sigaud and O. Buffet, *Markov Decision Processes in artificial intelligence*. John Wiley & Sons, 2013.
- [50] M. L. Puterman, *Markov Decision Processes: discrete stochastic dynamic programming*. John Wiley & Sons, 2014.

- [51] P. Sheng, G. Wang, K. Nayak, S. Kannan, and P. Viswanath, “BFT protocol forensics,” in *CCS*, 2021.
- [52] A. Shamis, P. Pietzuch, B. Canakci, M. Castro, C. Fournet, E. Ashton, A. Chamayou, S. Clebsch, A. Delignat-Lavaud, M. Kerner, J. Maffre, O. Vrousseau, C. M. Wintersteiger, M. Costa, and M. Russinovich, “IA-CCF: Individual accountability for permissioned ledgers,” in *NSDI*, 2022.
- [53] J. Neu, E. N. Tas, and D. Tse, “Ebb-and-Flow protocols: A resolution of the availability-finality dilemma,” in *S&P*. IEEE, 2021.
- [54] R. Neiheiser, M. Matos, and L. Rodrigues, “Kauri: Scalable BFT consensus with pipelined tree-based dissemination and aggregation,” in *SOSP*, 2021.
- [55] G. Danezis, L. Kokoris-Kogias, A. Sonnino, and A. Spiegelman, “Narwhal and Tusk: a DAG-based mempool and efficient BFT consensus,” in *Eurosys*, 2022.

## APPENDIX

Table IV: State transition and reward matrices for Streamlet.

State $\times$ Action	Resulting State	Pr.	$B_h$	$C$
$(cS, 0, l_h, H)$ Adopt	$(\min(cS+1, 3), 0, 1, A)$ $(\min(cS+1, 3), 0, 1, H)$	$\alpha$ $1-\alpha$	$l_h$	if $cS=2/3$ $C=1$
$(cS, 1, l_h, H)$ Adopt	$(1, 0, 1, A)$ $(1, 0, 1, H)$	$\alpha$ $1-\alpha$	$l_h$	
$(cS, 0, l_h, A)$ Adopt	$(cS, 1, 0, A)$ $(cS, 1, 0, H)$	$\alpha$ $1-\alpha$	$l_h$	
$(cS, 1, l_h, A)$ Adopt	$(0, 1, 0, A)$ $(0, 1, 0, H)$	$\alpha$ $1-\alpha$	$l_h$	
$(cS, 0, l_h, H)$ Wait, Silent	$(\min(cS+1, 3), 0, l_h+1, A)$ $(\min(cS+1, 3), 0, l_h+1, H)$	$\alpha$ $1-\alpha$	0	if $cS=2/3$ $C=1$
$(cS, 1, l_h, H)$ Wait, Silent	$(1, 0, l_h+1, A)$ $(1, 0, l_h+1, H)$	$\alpha$ $1-\alpha$	0	
$(cS, 0, l_h, A)$ Wait	$(0, 0, l_h, A)$ $(0, 0, l_h, H)$	$\alpha$ $1-\alpha$	0	
$(cS, 1, l_h, A)$ Wait	$(\min(cS+1, 3), 1, 0, A)$ $(\min(cS+1, 3), 1, 0, H)$	$\alpha$ $1-\alpha$	$l_h$	if $cS=2/3$ $C=1$
$(cS, 1, l_h, H)$ Release	$(\min(cS+2, 3), 0, 1, A)$ $(\min(cS+2, 3), 0, 1, H)$	$\alpha$ $1-\alpha$	$l_h$	(1)
$(cS, 1, l_h, A)$ Release	$(\min(cS+1, 3), 1, 0, A)$ $(\min(cS+1, 3), 1, 0, H)$	$\alpha$ $1-\alpha$	$l_h$	if $cS=2/3$ $C=1$
$(cS, 1, l_h, H)$ Withhold	$(0, 0, 0, A)$ $(0, 0, 0, H)$	$\alpha$ $1-\alpha$	$l_h$	
$(cS, 1, l_h, A)$ Withhold	$(\min(cS+1, 3), 1, 0, A)$ $(\min(cS+1, 3), 1, 0, H)$	$\alpha$ $1-\alpha$	$l_h$	if $cS=2/3$ $C=1$
$(cS, l_a, l_h, A)$ Silent	$(0, 0, 0, A)$ $(0, 0, 0, H)$	$\alpha$ $1-\alpha$	0	

(1) If  $cS=1$ ,  $C=1$ ; if  $cS=2/3$ ,  $C=2$

### A. Streamlet

Streamlet is a streamlined chained BFT protocol that is different from 2CHS, CHS and FHS. Firstly, it follows the longest certified chain rule, where an honest node only votes to the block that extends the longest certified chain. Due to this rule, the forking attack described in the main text will not appear in Streamlet. If the adversary tries to override an honest block, the honest nodes will not vote for it. However, the longest certified chain rule also introduces another way of attack. If the adversarial leader sends its proposal of block  $B$  to only part of  $(1/3 < \#honestnodes/\#nodes \leq 2/3)$  the honest nodes, excluding the next leader. The next leader does not see  $B$  and thus proposes a block  $B'$  at the same height

of  $B$ . After this new proposal, the adversarial nodes release their votes on  $B$ . At this point, honest nodes that previously received  $B$  will consider it the longest chain and will not vote for  $B'$ . We can consider this type of attack as preemptive forking attack. This difference will add a new action to the action space  $A$ .

Secondly, the lock and commit rules of Streamlet (referred to as notarize and final respectively in Streamlet) are different from the previous three protocols. Due to the broadcasting vote pattern, nodes can collect votes and generate QC locally at the end of each view. The block will be locked once certified. If a structure of three consecutive blocks is formed, the first two blocks will be committed. This difference will affect the reward allocation for  $B_h$  and  $C$ .

Moreover, Streamlet does not have view change step and is not responsive, so the time consuming in each view is the same, i.e.  $2\Delta$ . This mainly affects the reward distribution of  $T$ . The MDP modeling of Streamlet is shown in Table IV in detail.